This article has been published in Clinical Oral Investigations 20, 2411–2420. doi:10.1007/s00784-016-1738-y

Authors:

[1]Raquel Osorio.
[1]Inmaculada Cabello.
[2]Antonio L. Medina-Castillo.
[1]Estrella Osorio.
[1]Manuel Toledano.

Title:

Zinc-modified nanopolymers improve the quality of resin-dentin bonded interfaces.

Affiliations and addresses:

1. Dental School. University of Granada. Colegio Maximo, Campus de Cartuja s/n.18017 Granada, Spain.
2. NanoMyP. Spin-Off Enterprise from University of Granada. Edificio BIC-Granada. Av. Innovación1. 18016 Armilla, Granada, Spain.

Corresponding author:
Raquel Osorio
Dental School, University of Granada.
Colegio Maximo, Campus de Cartuja s/n 18017 Granada, Spain.
Phone: +34-958243793; Fax: +34-958240908.
E-mail: rosorio@ugr.es

Acknowledgments:

This work was supported by grant MINECO/FEDER MAT2014-52036-P. Authors do not have a financial relationship with the organization that sponsored the research.

Abstract

Demineralized collagen fibers at the hybrid layer are susceptible of degradation. Remineralization may aid to improve bond longevity. Objectives: to infiltrate zinc and calcium-loaded polymeric nanoparticles into demineralized dentin to facilitate hybrid layer remineralization. Materials and Methods: Zinc or calcium-loaded polymeric nanoparticles were infiltrated into etched dentin and Single Bond adhesive was applied. Bond strength was tested after 24 hours and six months storage. Nanomechanical properties, dye-assisted confocal laser microscopy and Masson's trichrome staining evaluation were performed to assess for the hybrid layer morphology, permeability and remineralization ability after 24 hours and three months. Data were analyzed by ANOVA and Student-Newman-Keuls multiple comparisons tests ($p<0.05$). Results: Immediate bond strength was not affected by nanoparticles infiltration (25 to 30 MPa), while after 6 months bond strengths were maintained (22 to 24 MPa). After 3 months, permeability occurred only in specimens in which nanoparticles were not infiltrated. Dentin remineralization, at the bottom of the hybrid layer, was observed in all groups. After microscopy analysis, zinc-loaded nanoparticles were shown to facilitate calcium deposition throughout the entire hybrid layer. Young's modulus at the hybrid layer increased from 2.09 to 3.25 GPa after 3 months, in specimens with zinc nanoparticles; meanwhile, these values were reduced from 1.66 to 0.49 GPa, in the control group. Conclusions: Infiltration of polymeric nanoparticles into demineralized dentin increased long-term bond strengths. Zinc-loaded nanoparticles facilitate dentin remineralization within the complete resin-dentin interface. Clinical Relevance: Resin-dentin bond longevity and dentin remineralization at the hybrid layer were facilitated by zinc-loaded nanoparticles.

Keywords: remineralization, zinc, nanopolymers, dentin, hybrid layer, adhesives.

INTRODUCTION

Dentin demineralization through acid etching and further resin infiltration are clinically required to promote resin-dentin bonding. During dentin demineralization, mineral ions are removed, resulting in exposure of the collagen matrix. Resin adhesive is further infiltrated into demineralized dentin and polymerized, to create the bonded interface called hybrid layer. The design of dental adhesives is focused on rendering a durable adhesion to dentin, and to protect the collagen fibrils at the hybrid layer, from degradation. If reincorporation of mineral into the demineralized dentin matrix is obtained, it may work as a site for further nucleation, and the newly remineralized tissue at the hybrid layer will be resistant to degradation [1].

Remineralization should be facilitated by restoring dentin with bioactive materials. To get ion-exchange and mineral precipitation within the hybrid layer, different particles have been incorporated into dental adhesives: bioactive glass, Portland cement or amorphous calcium phosphate [2,3,4]. However, minerals elute from the resins, producing a rapid decrease in their mechanical properties and bond strength [4]. At these conditions, ions liberation used to be rapid and not maintained overtime. A controllable release and optimal degradation kinetics are crucial but difficult to achieve [5].

Most of these tested materials have the ability of delivering calcium and phosphate ions to promote regrowth of remnant apatite crystals within the intrafibrillar zone of collagen fibrils (*via* classic nucleation) [6]. A second route to remineralization exists based upon biomineralization mediated by amorphous calcium and phosphate precursors (ACP) and polyanionic polymers [7].

Dentin infiltration with polymeric nanoparticles as a calcium and phosphate sequestering materials (i.e. carboxylate-functionalized polymer particles) previous to the bonding procedure has been proposed [8]. These polymers should bind to collagen and facilitate ACP precipitation at the hybrid layer. Nanopolymers may also act as carriers of other biological factors for the management of tissue mineralization [9, 10, 11]. Zinc can also be included at these particles in order to inhibit collagen degradation [12] and stimulate dentin remineralization [5, 13].

The aim of the present study was to infiltrate calcium or zinc-loaded polymeric nanoparticles into phosphoric acid etched dentin, prior to the adhesive application, in order to favor mineral precipitation to protect the hybrid layer, to maintain bond strengths in the long-term, and to recover mechanical properties at the previously demineralized hybrid layer. To ascertain for bond strength, mechanical recovery and mineral precipitation at the hybrid layer, different techniques were employed: a confocal laser microscopy (CLSM) analysis with a double-dying technique (rhodamine-B/fluoresceine) informs about the adhesive penetration, permeability and hybrid layer degradation at the bonded interface after 3 months [4,14]; microtensile bond strength was tested after 24 hours and 6 months in order to examine changes in the long-term bond strengths [2,4]. Dentin remineralization at the hybrid layer was assessed indirectly evaluating nanohardness increase at the hybrid layer, after 3 months of storage [2,4,14,6], and morphologically identifying calcium deposition by CLSM, using a selective mineral labeling dye [15]. A qualitative assessment of the collagen encapsulation was completed through Masson's trichrome staining, by observing color differences within the remineralized and non-remineralized interfacial zones after 3 months of storage [16,17].

The null hypotheses to be tested are that calcium and zinc-loaded nanoparticles infiltration, into etched dentin 1) does not affect long-term dentin bond strengths at the hybrid layer; and 2) do not facilitate remineralization at the demineralized bonded interface.

MATERIALS AND METHODS

Nanoparticles (NPs) production: PolymP-***n***Active NPs about 100 nm in diameter were purchased from NanoMyP (Granada, Spain). Particles are fabricated through polymerization precipitation. NPs composition is 2-hydroxyethyl methacrylate as a backbone monomer, ethylene glycol dimethacrylate as a cross-linker and methacrylic acid as a functional monomer. For zinc and calcium complexation, 30 mg of NPs were immersed at room temperature, during 3 days under continuous shaking in 15 ml of different aqueous solutions of $ZnCl_2$ or $CaCl_2$ (containing zinc or calcium at 40 ppm), in order to reach the adsorption equilibrium of metal ions. The pH of the suspensions was

adjusted to 6.5 with HCl or NaOH (0.1 M). Then, the suspensions were centrifuged (60 min, 12,000 rpm, two cycles) and the particles were separated from the supernatant [8]. Effective calcium and zinc complexation was monitored by optical emission spectrometry (ICP-OES Optima 8300, Perkin Elmer, MA, USA).

Microtensile bond strength (MTBS): 32 unerupted human third molars were employed with written informed consent from donors, under a protocol approved by the Institutional Review Board. Teeth were horizontally sectioned below the dentin-enamel junction and ground flat (180-grit). Dentin surfaces were treated following manufacturer instructions (phosphoric-acid etching, washing and drying). Before applying Single Bond (SB) resin (3M ESPE, St. Paul, MN, USA), an ethanol suspension of NPs, Zn-NPs, Ca-NPs (30 mg/ml) or just ethanol solution were applied (30 s) respectively, in each of the different experimental groups. Ethanol was gently evaporated for 30 s and finally SB resin was applied and a composite build-up was performed (TetricEvoCeram, Ivoclar-Vivadent, Schaan, Liechtenstein). Resin-bonded specimens were stored in deionized water at 37^{o} C for 24 h. Bonded tooth in each group (n=4) were sectioned into 10 beams (area: 1 mm^2). Beams were attached to a modified Bencor Multi-T testing apparatus (Danville Engineering Co., Danville, CA, USA) and tested to failure in tension, using a universal testing machine (Instron 4411; Instron Corporation, Canton, MA, USA) at a crosshead speed of 0.5 mm/min. Half of the specimens were tested at 24 h and the other half were stored and tested after 6 months. MTBS values were analyzed by two-way ANOVA including interactions analysis and Student-Newman-Keuls was used for multiple comparisons ($p<0.05$).

Field Emission Scanning Electron Microscopy analysis: Fractured specimens were examined with a stereomicroscope (Olympus SZ-CTV; Olympus, Tokyo, Japan) at 40x magnification to determine the mode of failure. Selected debonded dentin sticks were analyzed by Field Emission Scanning Electron Microscopy (FESEM) (GEMINI, Carl Zeiss SMT,Germany) at 2 to 3 KV and 3 to 3.5 mm working distance.

Nano-Indentation testing: 12 molars were cut and bonded as previously described (three specimens per group) and stored in PBS for 24 h. Teeth were longitudinally sectioned into slabs and polished using ascending grit SiC abrasive papers (#1200 to #4000) on a water-cooled polishing device (Buehler-MetaDi, Buehler Ltd. Lake Bluff, IL, USA) a

final polishing was performed using diamond pastes 1 to 0.25 μm. For each group, six slabs (two from each molar) were tested. An atomic force microscope (AFM-Nanoscope V, Digital Instruments, Veeco Metrology group, Santa Barbara, CA, USA) equipped with a Triboscope indentor system (Hysitron Inc., Minneapolis, MN) and a Berkovich indenter (tip radius ~20 nm) was employed for the nano-indentation processes, a liquid cell was used to guarantee a fully hydrated status of dentin during the complete procedure. On each slab, five indentation lines were executed in five different mesio-distal positions along the interface in a straight line starting from the adhesive layer down to the intertubular dentin. Indentations were performed with a load of 4000 nN and a time function of 10 s. The distance between each indentation was kept constant. Same specimens were tested at 24 h and after 3 months of storage. Young's Modulus values were analyzed by two-way ANOVA including interactions analysis and Student-Newman-Keuls was used for multiple comparisons ($p<0.05$).

Confocal Laser Microscopy analysis (CLSM): 48 further molars were bonded, as described above (twelve for each adhesive group). Previous to adhesive application, bond resin was doped with 0.05 wt% rhodamine-B (RhB, Sigma-Aldrich ChemieGmbh, Riedstr, Germany). Teeth were divided into two subgroups based on the period of storage in PBS (24 h or 3 months). Subsequent to the storage period, the specimens were further divided in another two subgroups (n=3), as two different dying techniques were used. In half of the specimens the pulpal chamber was filled with 1 wt% aqueous/ethanol fluorescein (Sigma-Aldrich ChemieGmbh, Riedstr, Germany) for 3 h [14]. The rest of the molars were immersed in 0.5 wt% xylenol orange solution (XO: Sigma-Aldrich ChemieGmbh, Riedstr, Germany), excited at 514-nm for 24 h at 37 ºC (pH 7.2). Specimens were copiously rinsed with water and treated in an ultrasonic water bath for 2 min. The specimens were cut in resin-dentin slabs and polished using ascending grit SiC abrasive papers (#1200 to #4000) on a water-cooled polishing device (Buehler-MetaDi, Buehler Ltd. Lake Bluff, IL, USA). A final ultrasonic cleaning (5 min) concluded the specimen preparation. Three specimens were analyzed for each study group with rhodamine/fluoresceine and other three with XO. Analysis of bonded interfaces were performed by dye assisted confocal microscopy evaluation, using a confocal laser scanning microscope equipped with 60x lenses (SP5 Leica, Heidelberg, Germany). As resins were doped with rhodamine, resin-diffusion and hybrid layer morphology was executed using rhodamine excitation laser. Rhodamine is excited using

green light (540 nm) and emits red in color (590 nm). Fluorescein was prefunded *ad retrum* trough the pulpar camera to ascertain for micropermeability and to detect non-protected collagen at the hybrid layer. Fluoresceine is activated by blue light (488-495 nm) and emits green/yellow (520 nm). CLSM images were obtained with a 1 μm z-step to optically section the specimens to a depth up to 12-10 μm below the surface. The z-axis scans of the interface surface was arbitrarily pseudo-colored by the same operator for better exposure and compiled into single projections using the Leica image-processing software SP2 (Leica, Heidelberg, Germany). The resolution of CLSM images was 1024 x 1024 pixels. Five optical images were randomly captured from each resin-dentin interface, and micrographs representing the most common features of nanoleakage observed along the bonded interfaces were selected. The configuration of the system was used at the same settings for the entire investigation. Micrographs representing the most common features observed along the bonded interfaces were recorded.

Masson's trichrome staining: 24 additional resin-dentin-bonded slices (six for each adhesive group) were used for the histomorphological evaluations. Teeth were divided into two subgroups based on the period of storage in PBS (24 h or 3 months). The medial aspects of each resin-dentin-bonded slice was fixed in a glass holder with a photocuring adhesive (Technovit 7210 VLC; Heraeus Kulzer GmbH Co., Werheim, Germany) and ground with SiC papers from 800 to 4,000 grits in a polisher (Apparatebau D-2000; Exakt Norderstedt, Germany) until its thickness was ~10 microns. Slices were stained with Masson's trichrome for differentiation of resin and non-resin encapsulation of the exposed collagen. This dye has a high affinity for cationic elements of normally mineralized type I collagen, resulting in staining collagen green, and when demineralized, resulting in different coloration, generally red; collagen coated with adhesive stains orange and pure adhesive appears beige. Slides with adherent stained sections were dehydrated through ascending ethanol and xylene. The sections were cover slipped and examined by light microscopy (BH-2; Olympus, Tokyo, Japan) at a 100× magnification. Two slices were prepared from each specimen, and images were digitized in a scanner (Agfa Twin 1200; Agfa-Gevaert NV, Mortsel, Belgium). In each specimen, the presence or absence of a red band corresponding to demineralized dentin was observed. A qualitative assessment of the collagen

encapsulation was completed by observing color differences within the interfacial zones of resin–dentin interfaces [16,17].

RESULTS

Microtensile bond strength: Mean MTBS values and modes of failure are reported in Table 1. After 24 h, MTBS values of tested groups were similar, mean and standard deviation (SD) values ranged from 25.55 (SD: 6.43) to 30.45 (SD: 4.22) MPa. After 6 months of storage, bond strength values only diminished in the group in which NPs were not applied; bond strength decreased from 30.45 (SD: 4.22) to 19.13 (SD: 3.03) MPa. After 6 months, attained mean values were maintained between 19.13 (SD: 3.03) and 24.11 (SD: 4.60) MPa, and no differences were found among groups. Most of the failures were mixed in all groups.

FESEM examination of debonded dentin surfaces revealed differences between groups (Figures 1A to 1H). In those groups infiltrated with NPs, collagen fibers integrity is maintained. Collagen is circumferentially oriented, constituting a normal dentin collagen network. In some cases, collagen fibers are showing the characteristic periodicity of cross striation (Figures 1D and 1F). At the contrary, in those cases in which NPs were not applied collagen fibers appeared denaturalized and fragmented (Figures 1A and 1B). A uniformly distributed but sparse mineral precipitation is observed at the intertubular dentin, on those dentin surfaces that were infiltrated with NPs (Figures 1C and 1D). Zn-NPs infiltrated dentin is showing a dense mineral phase formation, and most of the collagen is remineralized (Figures 1E and 1F). In those cases in which Ca-NPs were applied, it is difficult to see collagen fibrils, as a result of the dense mineral precipitation, both at the intertubular and intratubular dentin (Figures 1E and 1F).

Nano-Indentation testing: Mean Young's modulus values (GPa) and SD attained at the different indentation zones and time points, in the experimental groups are exposed in Table 2. No differences exist in mean values of elasticity between groups when Young's modulus was measured at the adhesive layer, values ranged from 2.43 (SD: 0.9) to 4.29 (SD:1.1) GPa; or at the underlying dentin, values were from 15.27 (SD:3.6) to 19.01 (SD:5.1) GPa. No changes in elasticity occurred at the adhesive layer or at the underlying dentin in any group, after the 3 months storage period. After 24 h, at the

bottom of the hybrid layer only a slight difference exist in nanoelasticity between the control (ethanol-resin) group (Mean: 6.15; SD:1.2 GPa) and the rest of the groups (ranging from 8.56; SD:2 to 9.1; SD:2 GPa). But after 3 months, except for the control all the experimental groups increase in mean elasticity, with values ranging from 13.06 (SD:3.5) to 16.24 (SD:3.8) GPa. At the hybrid layer no differences exist in elasticity between groups at 24 hours, but after 3 months experimental groups performed as follows: Ethanol (Mean:0.49; SD: 0.2 GPa) < NPs (Mean:1.93; SD:1.1 GPa) = Ca-NPs (Mean:1.80; SD:0.91 GPa) < Zn-NPs (Mean:3.25; SD:0.9 GPa).

Confocal Laser Microscopy analysis: The CLSM investigation showed that all the bonding procedures used in this study were able to create a resin diffusion zone within the demineralized dentin (hybrid layer 10–15 μm) and resin tags into the dentinal tubules. No traces of fluorescein penetration (permeability) were observed after 24 h (Figures 2A, 2B and 2C). Nevertheless, after 3 months clear signs of permeability and hybrid layer degradation were encountered at the primer/ethanol specimens (Figure 2E). In the group in which NPs were applied, fluoresceine penetrated but remained at the bottom of the hybrid layer, permeability through the hybrid layer was not produced (Figure 2F). When Zn-NPs or Ca-NPs were applied only a slight fluorescein penetration was observed within the hybrid layer, the minimum degree of permeability was observed at the Zn-NPs group (Figure 2G and 2H). It could be observed at XO-dyed specimens an active remineralization activity, both at 24h and after 3 months of storage. Remineralization was mainly produced at the walls of dentinal tubules and at the bottom of the hybrid layer, where resin is not present. Significant new calcium quelation was detected at the bottom of the hybrid layer, in all groups at any time point. Calcium quelation was not produced in zones in which resin was present (Figure 3). The group in which Zn-NPs were infiltrated did show a different remineralization pattern, the entire hybrid layer was incorporating calcium ions, intertubular and intratubular dentin mineralization was evidenced (Figure 3C and 3G).

Masson's trichrome staining: Representative images are shown in Figure 4. After 24 h, a limited red zone, representing resin uncovered and decalcified dentin was observed in all groups (Figure 4A, 4B, 4C and 4D). After 3 months of storage, an intense and wide red zone evidenced the existence of non-resin covered and demineralized dentin collagen (Figure 5). Active remineralization at the base of the hybrid layer was detected

in all groups. When NPs were not applied this band was wider than in the rest of the groups (Figure 4E and 4F). In the group in which Zn-NPs were applied a faint and non-continuous red line was found at the hybrid layer, green zones indicating intratubular and peritubular remineralization were observed within the hybrid layer (Figure 4I and 4J). When Ca-NPs were infiltrated only intratubular mineralization was observed at the hybrid layer (Figures 4K and 4L).

DISCUSION

The tested null hypotheses have to be partially rejected as polymeric nanospheres do not affect immediate bond strength but facilitate bond strength maintenance in the long-term, and zinc-loaded nanoparticles facilitate remineralization within the hybrid layer.

Bond strength was maintained overtime, only in those cases in which NPs were applied on etched dentin. When NPs were not applied, bond strength was reduced after 6 months of storage and collagen fibers appeared fragmented and morphologically altered at the debonded interface (Figures 1A and 1B). When NPs were applied the exposed collagen network was preserved after 6 months (Figures 1C, 1D, 1E and 1F). It is known, that collagen fibers are a relevant factor for the maintenance of normal tissue resistance. Collagen fibrils are hierarchically structured biological cables that serve as the principal tensile elements in tissues. Denatured collagen fibers with reduced mechanical properties are prone to fracture under tension [18], explaining the loose collagen fibrils encountered within the fractured hybrid layers in the resin-ethanol group (Figures 1A and 1B). How NPs may facilitate collagen preservation is not completely understood. It has been previously demonstrated, that NPs are able to inhibit dentin matrix metalloproteases, probably through a physical interaction and/or binding mechanism between the active-site zinc of MMPs and the acidic functional groups (COO^-) at NPs surfaces [8]. Loss of extra and intra-fibrillar mineral during dentin acid-etching exposes some gap regions within the collagen fibril and enables local telopeptidase activity to cleave C-terminal telopeptide, resulting in partial loss of intermolecular cross-links and collagen periodicity. As shown in figures 1D, 1F and 1H, in those groups in which NPs were applied, dentin collagen exhibited the typical 67 nm periodicity banding, and fibrils were not denatured or fractured. Moreover, in these

groups, fibrils had a high width (100 to 200 nm), which usually occurs when intrafibrillar mineralization exists or cross-linking is maintained [19].

Particle binding to demineralized collagen is produced (Figure 1D). It may be explained by: 1) the result of the high affinity between the negatively charged polymeric NPs (-43.3 mV) and the positively charged demineralized dentin collagen [20], or 2) due to the binding of COO^- groups from NPs to NH^+ sites at dentin collagen. Particle retention at the demineralized dentin surface is produced, it is important as NPs collagen binding is necessary to exert a remineralization effect [20, 21].

One of the main problems when incorporating calcium and phosphate containing particles into dental adhesives is to control for the calcium and phosphate release kinetic. Tested NPs may overcome this situation, as polymeric NPs do not dissolve or reabsorb, but are able to form amorphous calcium phosphate layer at their surface [8] and will remain attached to collagen fibrils, being incorporated into the remineralized tissue (Figure 1F and 1G). Therefore, NPs will facilitate mineral deposits formation. Carboxylate groups (COOH) may template the growth of calcium phosphates, as it has been previously shown in other different synthetic polymers [22,23]. If these formed mineral deposits will also facilitate a certain degree of intrafribrillar mineralization deserve future research. However, calcium and phosphate ions seem to be effective in dentin remineralization, where remaining mineral is present [7], as it occurs in partially demineralized dentin at the hybrid layer [24].

A double-dying technique (rhodamine-B/fluoresceine) was employed to study adhesive penetration and permeability at the bonded interface [14], by means of CLSM. Adhesive penetration is assessed by the resin doped with rhodamine. In all groups, similar features (thick hybrid layers and numerous resin tags) are encountered, and micropermeability is not evidenced in any group. It indicates that NPs do not alter adhesive penetration or hybrid layer formation (Figure 2) [8]. After 3 months of storage, fluoresceine is detectable in the resin-ethanol group (in which NPs were not applied), and fluoresceine permeates through the hybrid layer creating a yellow band at the adhesive layer (Figure 2E). It clearly indicates that permeability exists. It is a sign of hybrid layer degradation. Fluoresceine molecules [$C_20H_{12}O_5$] contains reactive -COOH and -OH groups acting as labeling agent to preferentially stain demineralized and non-

resin covered dentin collagen through hydrogen bonding to the hydroxyl groups of collagen or by covalent bonding between the NH groups of collagen and the COOH, OH and C=O groups of fluorescein [25]. In the group in which NPs were applied the bottom of the hybrid layer is stained by fluoresceine but it did not permeate through the hybrid layer, which maintained an adequate sealing (Figure 2F). Zn-NPs and Ca-NPs groups did not show fluoresceine staining or filtration trough the hybrid layer. These findings are in accordance to attained MTBS values and FESEM images, as bond strength was maintained and degradation of collagen was not observed in those groups in which NPs were applied.

Dentin mineralization at the hybrid layer has been previously assessed by different techniques (morphological, chemical, or mechanical) but mostly analyzed at the specimen surface [2,4,14]. CLSM, even when it has low image resolution, permits deep tissue imaging, and may provide a useful method if combined with a selective mineral labeling dye [15]. Xylenol orange dye was selected for mineralization analysis as it is fixed in newly formed calcified tissues where it remains until removal of the mineral. Xylenol orange forms complexes with divalent ions from calcium, producing an orange fluorescence and it is found in tissues which were calcifying at the time of administration (i.e. those parts of the bonded interface at which mineralization is taking place) [26]. Mineralization is found in all groups at the bottom of the hybrid layer, were adhesive resin is not infiltrated (Figure 3), Masson's trichrome staining results did also confirm this fact (Figure 4), it has been previously shown that zones within the hybrid layer that were well-infiltrated by adhesive resin did not undergo remineralization [27]. So remineralization was only expected at zones in which an incomplete resin infiltration occurred [28]. As most currently employed dimethacrylate resin formulations posse restricted levels of conversion within the hybrid layer, a significant amount of free monomer remains unreacted, and is potentially degradable [29]. Even when signs of remineralization are ascertained, a functional remineralization of the acid-etched resin-bonded dentin is only considered if an increase of the modulus of elasticity is produced within the bonded interfaces [30,14]. In accordance to the Masson's trichrome staining and CLSM analyses of the tested bonded interfaces, there are evidences of functional remineralization at the bottom of the hybrid layer in all experimental groups in which NPs were applied, and mechanical properties also increased after 3 months of storage (Table 2). Integrity of the collagen fibres at the bottom of the hybrid layer was

evidenced, when the debonded interfaces were examined by FESEM, after 6 months (Figures 1C to 1H). In the control group, fractured collagen fibres were observed (Figures 1A and 1B), what may be due to collagen degradation by endogenous dentin proteases, as explained above.

There is a clear need to improve bioactivity (capability of CaP deposition) of our dental adhesive systems. The tested Zn-doped NPs seem to offer exciting possibilities, as calcium quelation (Xylenol orange fixation) is produced throughout the entire hybrid layer (Figure 3C and 3G). After Masson's trichrome staining intratubular and intertubular mineralization thorough the complete bonded interface were also probed (Figure 4I and 4J). In a previous study, a ZnO-doped resin was shown to exhibit bioactivity, forming calcium and phosphate deposits after 7 days of immersion in simulated body fluid solution. Under immersion Zn-OH groups are formed, and these Zn-OH groups are able to induce phosphate and calcium ions deposition [31].

It has to be stressed that results based upon the microscopic images have to be taken with caution, as presented pictures are only exemplary and may leave room for speculation. They provide a qualitative assessment and they must only be considered besides the performed quantitative analysis. In this study, mechanical properties at the hybrid layer were measured after 24 h and 3 months (Table 2). Significant increases in Young's modulus were encountered at the hybrid layer, when using the experimental zinc-NPs, and it did not occur in the other experimental groups, corroborating the previously described findings after trichrome staining and the dye-assisted CLSM analysis of these bonded interfaces. It is meaningful, even when values did not reach the level of natural mineralized or intact dentin [32]. The association between mineral precipitation and metalloproteinases inhibition induced by zinc doped adhesives has been previously published. It has been concluded that zinc doped dentin adhesives may have therapeutic/protective effects for stabilizing etch-and rinse hybrid layers [32].

When NPs were applied and Xylenol-stained interfaces were observed after 24 h, a continuing calcium quelation at the resin infiltrated dentin was also observed, which may be due to the high calcium complexation ability of the tested NPs [8], however, this effect was not observable on dyed specimens, after 3 months of storage.

Remineralization may be ascertained, between others, by means of changes in mechanical properties (nanoindentation) [2,4,14], changes in mineral composition (RAMAN spectroscopy, X-ray difraction, EDX or FT-IR spectroscopy analyses) [14,15], and changes in histomorphological and microstructural appearance assessed through microradiography, μCT, atomic force microscopy, scanning probe microscopy, scanning electron microscopy, transmission electron microscopy, dye assisted optical or confocal microscopy [4,14]. Even when some correlation between all these analyses has usually been found, some of them are complementary. Therefore, this study presents certain limitations and further research is required. The significance of the encountered differences in mineral apposition at the hybrid layer, between the tested groups, may have a degree of uncertainty associated with the interpretation of the presented low resolution fluorescent images; transmission electron microscopy associated to a diffraction analysis is compulsory to ascertain for true intrafibrillar collagen remineralization at the hybrid layer. Furthermore, a chemical characterization of the produced changes at the bonded interfaces by RAMAN or FT-IR analyses is also desirable to confirm for mineral gain. There is also a need to conduct clinical studies in order to corroborate findings of the present in vitro study.

It has been demonstrated that usually employed hydrophobic resins are not able to protect the exposed collagen fibrils effectively, and water and enzymes can facilitate hydrolytic degradation of the hybrid layer [33]. Therefore, the science of engineered nanoparticles offers strategies to help with the maintenance and remineralization of collagen in acid-treated dentin, as non-reabsorbible carriers for bioactive ions (e.g. Ca, P or Zn), and should also expand toward the encapsulation of other therapeutic agents [34], deserving future research.

CONCLUSIONS

i) Infiltration of polymeric nanoparticles into demineralized dentin provided maintenance of bond strengths in the long-term and collagen preservation at the hybrid layer.

ii) Zn-loaded nanoparticles facilitate calcium deposition and induce an increase in mechanical properties at the hybrid layer, after 3 months of storage.

REFERENCES

1. Liu Y, Tjäderhane L, Breschi L, Mazzoni A, Li N, Mao J, Pashley DH, Tay FR (2011) Limitations in bonding to dentin and experimental strategies to prevent bond degradation. J Dent Res 90: 953-968. doi: 10.1177/0022034510391799

2. Sauro S, Osorio R, Watson TF, Toledano M (2012) Therapeutic effects of novel resin bonding systems containing bioactive glasses on mineral-depleted areas within the bonded-dentine interface. J Mater Sci Mater Med 23:1521-1532. doi: 10.1007/s10856-012-4606-6.

3. Osorio R, Yamauti M, Sauro S, Watson TF, Toledano M (2014) Zinc incorporation improves biological activity of beta-tricalcium silicate resin-based cement. J Endod 40:1840-1845. doi: 10.1016/j.joen.2014.06.016

4. Sauro S, Osorio R, Osorio E, Watson TF, Toledano M (2013) Novel light-curable materials containing experimental bioactive micro-fillers remineralise mineral-depleted bonded-dentine interfaces. J Biomater Sci Polym Ed 24: 940-956. doi: 10.1080/09205063.2012.727377

5. Hoppe A, Güldal NS, Boccaccini AR (2011) A review of the biological response to ionic dissolution products from bioactive glasses and glass-ceramics. Biomaterials 32: 2757-2774. doi: 10.1016/j.biomaterials.2011.01.004

6. Kinney JH, Habelitz S, Marshall SJ, Marshall GW (2003) The importance of intrafibrillar mineralization of collagen on the mechanical properties of dentin. J Dent Res 82: 957-961. doi: 10.1177/154405910308201204

7. Thompson VP, Watson TF, Marshall GW Jr, Blackman BR, Stansbury JW, Schadler LS, Pearson RA, Libanori R (2013) Outside-the-(cavity-prep)-box thinking. Adv Dent Res 25: 24-32. doi: 10.1177/0022034513502207

8. Osorio R, Osorio E, Medina-Castillo AL, Toledano M (2014) Polymer nanocarriers for dentin adhesion. J Dent Res 93:1258-1263. doi: 10.1177/0022034514551608

9. Leonor IB, Balas F, Kawashita M, Reis RL, Kokubo T, Nakamura T (2009) Biomimetic apatite deposition on polymeric microspheres treated with a calcium silicate solution. J Biomed Mat Res B Appl Biomat 91: 239-247. doi: 10.1002/jbm.b.31395.

10. Wu C, Zhang Y, Fan W, Ke X, Hu X, Zhou Y, Xiao Y (2011) CaSiO3 microstructure modulating the in vitro and in vivo bioactivity of poly(lactide-co-glycolide) microspheres. J Biomed Mater Res Part A 98A: 122-131. doi: 10.1002/jbm.a.33092.

11. Musyanovych A, Landfester K (2014) Polymer Micro- and Nanocapsules as Biological Carriers with Multifunctional Properties. Macromol Biosci 14: 458-477. doi: 10.1002/mabi.201300551.

12. Osorio R, Yamauti M, Osorio E, Ruiz-Requena ME, Pashley DH, Tay FR, Toledano M (2011) Zinc reduces collagen degradation in demineralized human dentin explants. J Dent 39: 148-153. doi: 10.1016/j.jdent.2010.11.005

13. Lynch RJ, Churchley D, Butler A, Kearns S, Thomas GV, Badrock TC, Cooper L, Higham SM (2011) Effects of Zinc and Fluoride on the Remineralisation of Artificial Carious Lesions under Simulated Plaque Fluid Conditions. Caries Res 45: 313-322. doi: 10.1159/000324804.

14. Sauro S, Osorio R, Watson TF, Toledano M (2015) Influence of phosphoproteins' biomimetic analogs on remineralization of mineral-depleted resin-dentin interfaces created with ion-releasing resin-based systems. Dent Mat 31: 759-777. doi: 10.1016/j.dental.2015.03.013.

15. Profeta AC, Mannocci F, Foxton R, Watson TF, Feitosa VP, De Carlo B, Mongiorgi R, Valdré G, Sauro S (2013) Experimental etch-and-rinse adhesives doped with bioactive calcium silicate-based micro-fillers to generate therapeutic resin-dentin interfaces. Dent Mater 29:729-741. doi: 10.1016/j.dental.2013.04.001.

16. Toledano M, Aguilera FS, Osorio E, Cabello I, Toledano-Osorio M, Osorio R (2015) Self-etching zinc-doped adhesives improve the potential of caries-affected dentin to be functionally remineralized. Biointerphases 15;10:031002. doi: 10.1116/1.4926442.

17. Toledano M, Aguilera FS, Osorio E, Cabello I, Osorio R (2014) Microanalysis of thermal-induced changes at the resin-dentin interface. Microsc Microanal 20: 1218-1233. doi: 10.1017/S1431927614000944

18. Tay FR, Carvalho RM, Yiu CK, King NM, Zhang Y, Agee K, Bouillaguet S, Pashley DH (2000) Mechanical disruption of dentin collagen fibrils during resin-dentin bond testing. J Adhes Dent 2:175-192.

19. Bertassoni LE, Habelitz S, Pugach M, Soares PC, Marshall SJ, Marshall GW Jr (2010) Evaluation of surface structural and mechanical changes following remineralization of dentin. Scanning 32: 312-319. doi: 10.1002/sca.20199

20. Besinis A, van Noort R, Martin N (2012) Infiltration of demineralized dentin with silica and hydroxyapatite nanoparticles. Dent Mater 28: 1012-1023. doi: 10.1016/j.dental.2012.05.007.

21. Besinis A, van Noort R, Martin N (2014) Remineralization potential of fully demineralized dentin infiltrated with silica and hydroxyapatite nanoparticles. Dent Mater 30: 249-262. doi: 10.1016/j.dental.2013.11.014.

22. Li J, Yang J, Li J, Chen L, Liang K, Wu W, Chen X, Li J (2013) Bioinspired intrafibrillar mineralization of human dentine by PAMAM dendrimer. Biomaterials 34: 6738-6747. doi: 10.1016/j.biomaterials.2013.05.046

23. Song J, Malathong V, Bertozzi CR (2005) Mineralization of synthetic polymer scaffolds: a bottom-up approach for the development of artificial bone. J Am Chem Soc 16;127(10):3366-3372. doi: 10.1021/ja043776z

24. Toledano M, Osorio E, Cabello I, Osorio R (2014b) Early dentine remineralisation: morpho-mechanical assessment. J Dent 42: 384-394. doi: 10.1016/j.jdent.2014.01.012.

25. Zhang Y, Yuan Y, Liu C (2008) Fluorescent labeling of nanometer hydroxyapatite. J Mater Sci Technol 24:187-191.

26. Rahn BA, Perren SM (1971) Xylenol orange, a fluorochrome useful in polychrome sequential labeling of calcifying tissues. Stain Technol 46: 125-129.

27. Niu LN, Zhang W, Pashley DH, Breschi L, Mao J, Chen JH, Tay FR (2014) Biomimetic remineralization of dentin. Dent Mater 30: 77-96. doi: 10.1016/j.dental.2013.07.013.

28. Kim J, Mai S, Carrilho MR, Yiu CK, Pashley DH, Tay FR (2010) An all-in-one adhesive does not etch beyond hybrid layers. J Dent Res 89:482-487. doi: 10.1177/0022034510363665.

29. Stansbury JW, Dickens SH (2001) Network formation and compositional drift during photo-initiated copolymerization of dimethacrylate monomers. Polymer 42: 6363-6369. doi:10.1016/S0032-3861(01)00106-9.

30. Bertassoni LE, Habelitz S, Marshall SJ, Marshall GW (2011) Mechanical recovery of dentin following remineralization in vitro–an indentation study. J Biomech 44: 176-181. doi: 10.1016/j.jbiomech.2010.09.005.

31. Osorio R, Cabello I, Toledano M (2014) Bioactivity of zinc-doped dental adhesives. J Dent 42:403-412. doi: 10.1016/j.jdent.2013.12.006

32. Toledano M, Sauro S, Cabello I, Watson T, Osorio R (2013) A Zn-doped etch-and-rinse adhesive may improve the mechanical properties and the integrity at the bonded-dentin interface. Dent Mater 29:142-152. doi: 10.1016/j.dental.2013.04.024.

33. De Munck J, Mine A, Vivan Cardoso M, Van Landuyt KL, Lührs AK, Poitevin A, Hanabusa M, Kuboki T, Van Meerbeek B (2013) Hydrolytic stability of three-step etch-and-rinse adhesives in occlusal class-I cavities. Clin Oral Investig 17:1911-1918. doi: 10.1007/s00784-012-0884-0

34. Alkatheeri MS, Palasuk J, Eckert GJ, Platt JA, Bottino MC (2015) Halloysite nanotube incorporation into adhesive systems-effect on bond strength to human dentin. Clin Oral Investig 19:1905-1912. doi: 10.1007/s00784-015-1413-8.

Table 1. Mean and standard deviation of microtensile bond strength (MPa) to dentin and mode of failure of the different experimental groups after 24 h and three months storage periods.

	MTBS Mean (SD)		Mode of failure(%) [A/C/M]	
	24 hours	**6 months**	**24 hours**	**6 months**
Ethanol + Resin	30.45 (4.22) a1	19.13 (3.03) A2	[0/0/100]	[30/0/70]
NPs + Resin	26.09 (4.53) a1	21.82 (3.54) A1	[10/0/90]	[18/0/82]
Zn-NPs + Resin	26.58 (5.43) a1	24.11 (4.60) A1	[4/0/96]	[3/2/95]
Ca-NPs + Resin	25.55 (6.43) a1	22.87 (4.28) A1	[7/0/93]	[8/2/90]

Abbreviations. MTBS: microtensile bond strength to dentin. SD: standard deviations. NPs: nanoparticles. Zn-NPs: zinc-loaded nanoparticles. Ca-NPs: calcium-loaded nanoparticles.
[A/C/M]: [adhesive/cohesive/mixed].
Letters indicate no significant difference in vertical columns and numbers in rows using Student-Newman-Keuls test ($p<0.05$).

Table 2. Mean and standard deviation (SD) of Young's modulus of elasticity (Ei) in GPa, at the different experimental bonded interfaces, after 24 hours and 3 months storage periods.

Ethanol + Resin	**24 hours**	**3 months**
Adhesive layer	2.43 (0.9) 1a	2.44 (1.2) 1a
Hybrid layer	1.66 (0.5) 1a	0.49 (0.2) 2a
Bottom hybrid layer	6.15 (1.2) 1a	7.08 (1.8) 1a
Underlying dentin	16.66 (3.1) 1a	15.27 (3.6) 1a
NPs + Resin	**24 hours**	**3 months**
Adhesive layer	3.53 (1) 1a	3.1 (1) 1a
Hybrid layer	2.15 (1.1) 1a	1.93 (1.1) 1b
Bottom hybrid layer	8.56 (2) 1ab	13.06 (3.5) 2b
Underlying dentin	15.93 (2.8) 1a	16.56 (4.3) 1a
Zn-NPs + Resin	**24 hours**	**3 months**
Adhesive layer	3.75 (0.8) 1a	3.17 (0.7) 1a
Hybrid layer	2.09 (0.5) 1a	3.25 (0.9) 2c
Bottom hybrid layer	8.81 (2.6) 1ab	14.12 (3.8) 2b
Underlying dentin	16.32 (3.3) 1a	17.24 (4.2) 1a
Ca-NPs + Resin	**24 hours**	**3 months**
Adhesive layer	4.17 (1) 1a	4.29 (1.1) 1a
Hybrid layer	2.28 (1.3) 1a	1.80 (0.91) 1b
Bottom hybrid layer	9.1 (2) 1b	16.24 (3.8) 2b
Underlying dentin	19.01 (5.1) 1a	18.55 (5.5) 1a

Abbreviations. NPs: nanoparticles. Zn-NPs: zinc-loaded nanoparticles. Ca-NPs: calcium-loaded nanoparticles. Letters indicate no significant difference in vertical columns within the same indentation zone and numbers in rows using Student-Newman-Keuls test ($p<0.05$).

FIGURE LEGENDS

Figure 1. Field emission scanning electron microscopy images of debonded resin-dentin specimens tested after 6 months of artificial saliva storage. **A)** Debonded dentin surface after bonding with SB and water/ethanol as primer. Dentinal tubules with fractured resin tags (arrows) and demineralized collagen fibers are visible. **B)** At a higher magnification, fractured collagen fibers that are not mineralized o resin protected are apparent. Collagen fibers show loose ends, a reduced diameter and seem to be disrupted. **C** and **D)** Dentin surface in which NPs were infiltrated before bonding, denuded collagen fibers and some fractured resin tags are detected inside dentinal tubules (asterisks). Collagen fibers are organized and non-fractured, exhibiting diameters above 100 microns and characteristic periodical striation (arrows). **E** and **F)** Debonded dentin surface where Zn-NPs infiltration was performed before bonding. Intertubular dentin is observed, with a dense collagen network in which fibrils exhibit a growing width (100 to 200 nm), and the typical 67 nm periodicity (arrows). NPs may be seen attached to collagen fibres (open arrows). Some tubules are evident (asterisks). Mineral deposits are patent. **G)** and **H)** Dentin surface in which Ca-NPs were infiltrated. A dense layer of mineral deposits is visible at the intertubular dentin. Some tubules are partially or totally occluded by minerals (asterisks). Some collagen fibers are observable showing a normal diameter a characteristic striation (arrows). NPs are hardly distinguished (open arrows).

Figure 2. CLSM images of the resin-dentin interfaces. CLSM single projection after 24 h of the resin-dentin interface created **A)** without NPs application, **B)** after NPs infiltration in etched dentin, **C)** when Zn-NPs were applied and **D)** after using Ca-NPs. Proper adhesive penetration and resin tags formation is observed in all cases. Fluoresceine was not present, indicating adequate resin infiltration of the etched dentin. Just slight traces of fluoresceine are evident when no NPs were applied (arrow), but fluoresceine did not pass through the hybrid layer. At CLSM images of the resin-dentin interfaces performed after 3 months of storage, it is possible to note the presence of fluoresceine emission. **E)** When no NPs were applied, fluoresceine was able to pass through the hybrid layer creating a continuous line of emission (arrows) at the adhesive layer (al) it indicates the existence of a degraded hybrid layer. Remnant resin tags are present (rt) but seems to be degraded at the top of the hybrid layer. **F)** In the specimens

in which NPs were applied, a wide band of fluoresceine emission is observed (between arrows), it is important to note that fluoresceine did not reach the top of the hybrid layer and remain at the demineralized collagen in the intertubular dentin. Resin tags (rt) are funnel shaped and thick at the base, indicating absence of degradation**. G and H)** When Zn-NPs or Ca-NPs were applied respectively, just a slight trace of fluoresceine emission is observed, and no signs of micropermeability are shown (fluoresceine did not pass through the hybrid layer). Resin tags (rt) are numerous, thick and funnel shaped. A non-degraded and correctly sealed hybrid layer is then observed for both groups. Scale bar is 10 microns

Figure 3. CLSM single-projection images disclosing the fluorescence after the calcium chelator dye xylenol orange application. **A**, **B**, **C** and **D** correspond to the images obtained after 24 h evaluation, at the different experimental groups in the following order: no NPs, NPs, Zn-NPs and Ca-NPs. **E**, **F**, **G** and **H** are images obtained from 1m stored specimens (same order). In all groups and at any time point signals of orange stain were observed at the bottom of the hybrid layer (bhl) where resin is not present, and walls of the dentinal tubules appeared also clearly stained with the calcium chelator dye. A remarkable and differential fluorescence signal was shown throughout the entire hybrid layer (asterisks) when Zn-NPs were applied and interfaces were evaluated after 24 h **(C)** or after 3 months **(G**) and in the group in which NPs were applied and interfaces evaluated after 24 h (**B**). Scale bar is 10 microns

Figure 4. Representative light micrographs of the interface specimens stained with Masson's trichrome. Mineralized dentin stained green/blue, adhesive stained beige, and exposed protein stained red. **A, B, C and D)** Bonded resin-dentin interfaces, stained after 24 h of storage, without NPs, after NPs, Zn-NPs and Ca-NPs infiltration respectively. A limited fringe of exposed collagen is observed at the hybrid layer in all groups. Scale bar is 10 microns. **E and F)** Bonded dentin interfaces without NPs, after 3 months of storage. A wide zone of exposed demineralized collagen is observed. Scale bars are 10 and 4 microns respectively. **G** and **H)** Resin-dentin interfaces bonded after NPs infiltration into dentin, and stained after 3 months of storage. Exposed collagen is patent but there is a mineralization front at the base of the hybrid layer limiting its wideness. Scale bars are 10 and 4 microns respectively. **I** and **J)** Bonded resin-dentin interfaces with Zn-NPs infiltration, after 3 months of storage are shown. The

demineralization zone is discontinuous and remineralization is occurring at the intratubular and peritubular dentin (arrow). Scale bars are 10 and 4 microns respectively. **K** and **L)** Resin-dentin interfaces bonded after Ca-NPs infiltration into dentin (after 3months of storage). A remineralized fringe at the bottom of the hybrid layer is noticed and initial intratubular mineralization (arrow) may also be observed at the hybrid layer. Scale bars are 10 and 4 microns respectively.

COMPLIANCE WITH ETHICAL STANDARDS:

Funding: This study was funded by Ministerio Español de Economía y Competitividad, grant number MINECO/FEDER MAT2014-52036-P. Authors do not have a financial relationship with the organization that sponsored the research.

Conflict of Interest: Raquel Osorio declares that she has no conflict of interest. Inmaculada Cabello declares that she has no conflict of interest. Antonio L. Medina-Castillo declares that he has no conflict of interest. Estrella Osorio declares that she has no conflict of interest. Manuel Toledano declares that he has no conflict of interest.

Ethical approval: All procedures performed in the present study, involving human participants, were in accordance with the ethical standards of the institutional and/or national research committee and with the 1964 Helsinki declaration and its later amendments or comparable ethical standards. This article does not contain any studies with animals performed by any of the authors.

Informed consent: Informed consent was obtained from all individual participants included in the study.

Figure 1

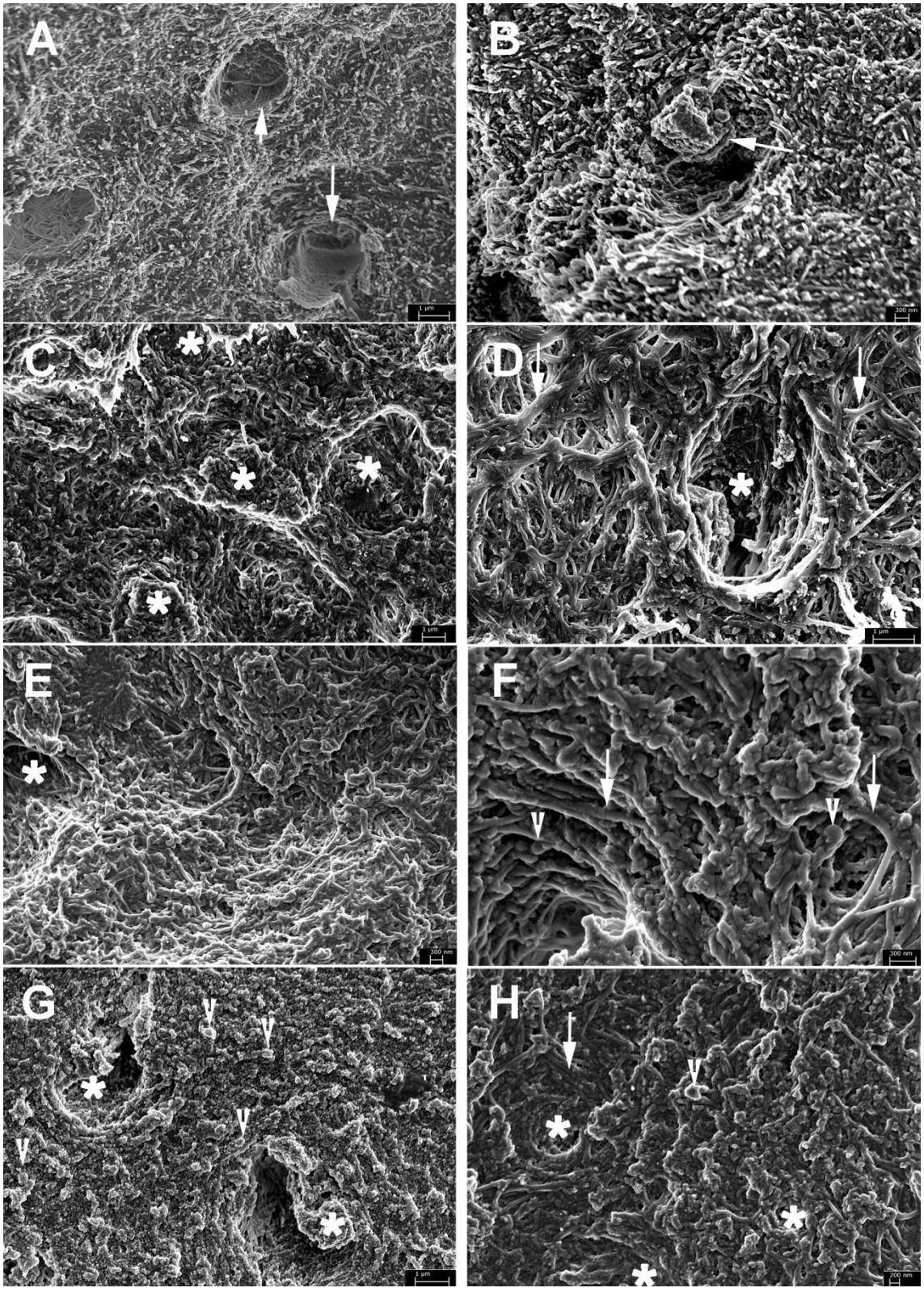

Figure 2

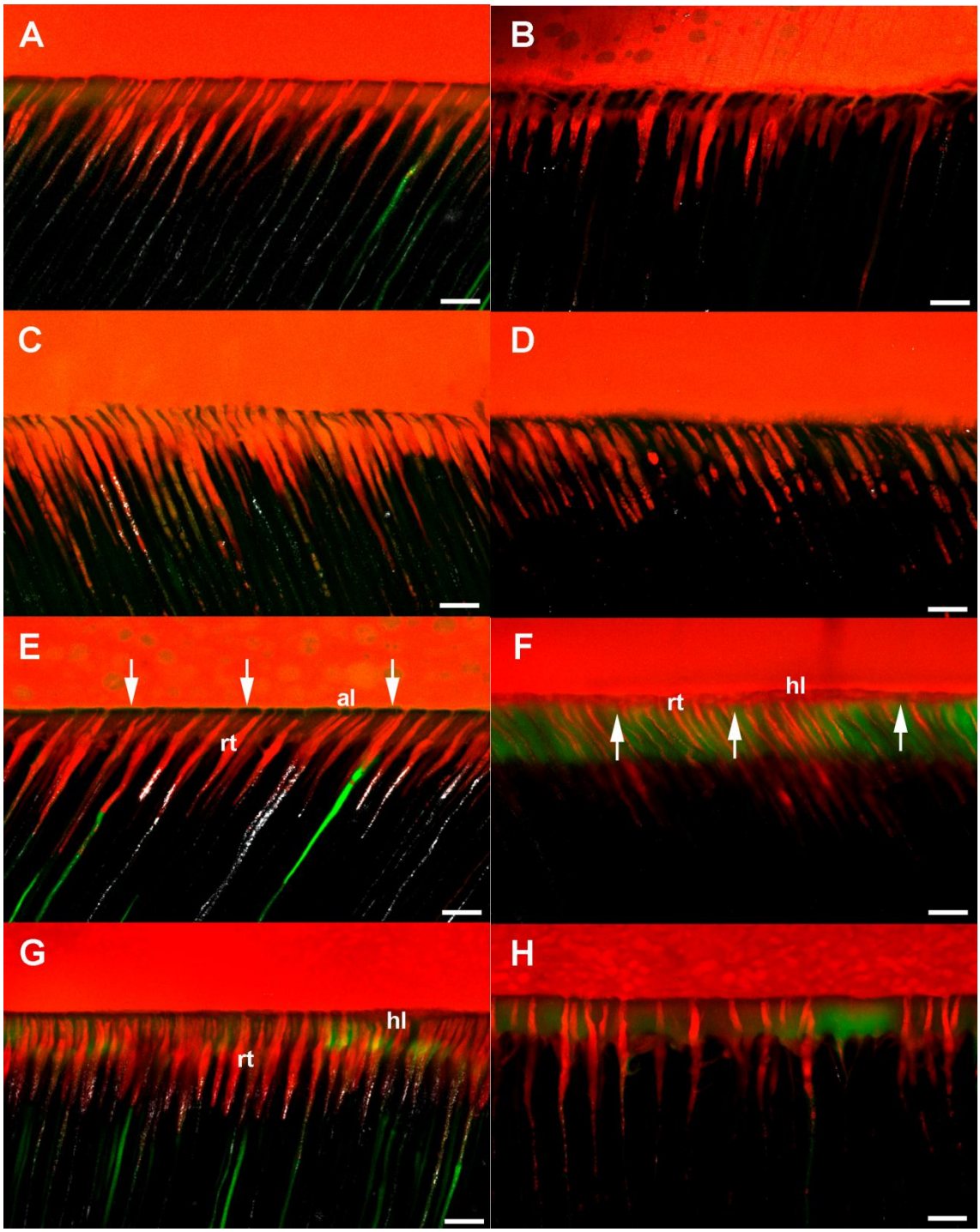

Figure 3

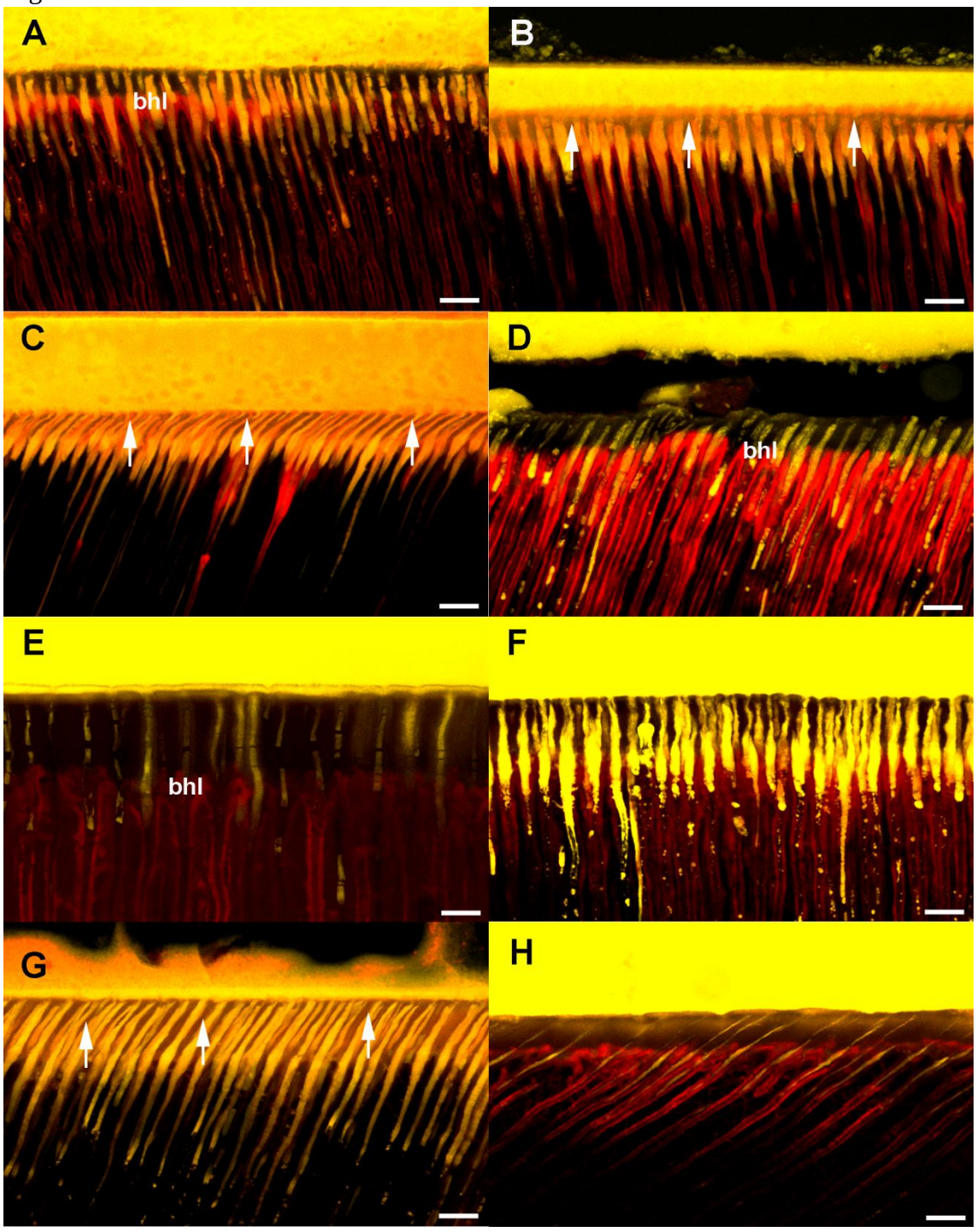
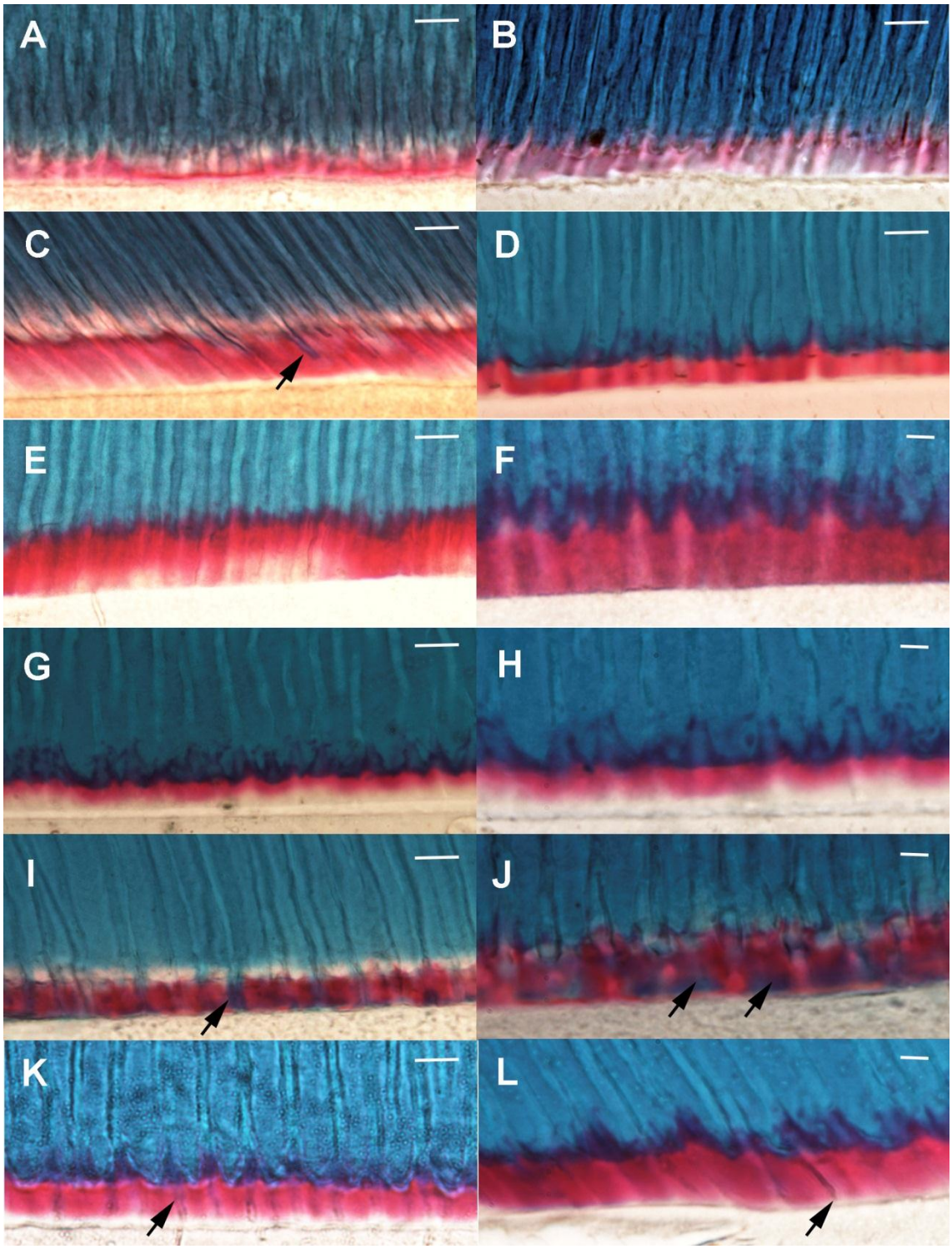
Figure 4